Ohmic contact-free mobility measurement in ultra-wide bandgap AlGaN/AlGaN devices

Peter A. Butler, William M. Waller, Michael J Uren, *Member, IEEE,* Andrew Allerman, Andrew Armstrong, Robert Kaplar, *Senior Member, IEEE,* and Martin Kuball, *Senior Member, IEEE*

***Abstract*—We measure the electron density dependence of carrier mobility in ultra-wide bandgap $Al_{0.85}Ga_{0.15}N/Al_{0.7}Ga_{0.3}N$ heterostructures, using only Au/Pt Schottky contact deposition and without the need for Ohmic contacts. With this technique, we measure mobility over a 2DEG density range from $10^{10} - 10^{13}$ cm^{-2} at an AlGaN/AlGaN heterojunction. At room temperature subthreshold mobility was 4 cm^2/Vs and peak mobility 155 cm^2/Vs. Peak mobility decreased with temperature as $T^{-0.86}$ suggesting alloy scattering as the dominant scattering mechanism.**

***Index Terms*—AlGaN, mobility, Ohmic contact, Schottky.**

I. Introduction

ULTRA-wide bandgap (UWB) heterojunctions enable higher breakdown voltage capability than the more common AlGaN/GaN field effect transistor devices [1], however, mobility may be a performance limiting factor due to alloy scattering in a ternary channel. Established methods to determine the channel sheet charge density dependence of mobility in devices include field effect mobility and Hall mobility [2]. Such techniques are often limited to measuring mobility in the unbiased case, i.e. at one carrier density, or over a narrow range of carrier density. Gated Hall techniques have been used to measure mobility in AlGaN/GaN structures over almost a decade span of carrier density, e.g. Manfra measured mobility from $2 \times 10^{11} - 2 \times 10^{12}$ cm^{-2} [3], where it was found that $\mu \propto n_{2DEG}$, due to scattering from charged dislocations limiting mobility [4]. The gated Hall measurement required insulated gate Hall bars to be fabricated, and a magnetic field applied. In contrast, gate admittance techniques [5] provide mobility data over a much wider carrier density range, using simpler test structures and equipment.

Ohmic contact formation in ultra-wide bandgap semiconductors remains difficult, making FET based mobility measurements challenging. In this work, we demonstrate a technique for measuring mobility without the need for Ohmic contact formation. The technique is suitable for use in characterising mobility in semiconductor materials, and requires only Schottky metal deposition. Using this technique we extract the 2DEG mobility of an UWB device from the weak inversion regime through to the strong inversion unbiased case for the first time. We show that mobility temperature dependence measurements and 2DEG density dependence measurements indicate alloy scattering is the dominant mechanism.

This work was supported by the AWE Technical Outreach Fund, the Sandia National Laboratories Ultra-Wide Bandgap Power Electronics Grand Challenge LDRD, and the Engineering and Physical Sciences Research Council (EPSRC) under grant number EP/L007010/1. Sandia National Laboratories is a multimission laboratory managed and operated by National Technology and Engineering Solutions of Sandia, LLC., a wholly owned subsidiary of Honeywell International, Inc., for the U.S. Department of Energy's National Nuclear Security Administration under contract DE-NA-0003525.

P.A. Butler, W.M. Waller, M.J. Uren, and M. Kuball are with the Centre for Device Thermography and Reliability, H. H. Wills Physics Laboratory, University of Bristol, United Kingdom. P.A.B. is also with AWE Plc., Aldermaston, Reading, United Kingdom. e-mail: Peter.Butler@Bristol.ac.uk

A. Allerman, A. Armstrong, and R. Kaplar are with Sandia National Laboratories, Albuquerque, New Mexico, USA.

Manuscript received 26th September, 2017; revised 3rd November, 2017.

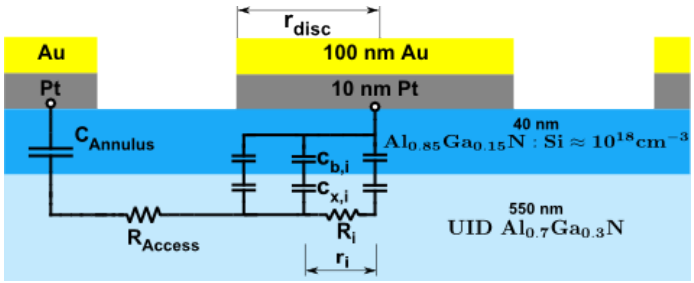

Fig. 1. Schematic of the equivalent circuit model used for the analysis of the experimental data obtained from the disc-annulus structure. The disc is modelled as a complex impedance constructed from finite elements, each consisting of a resistance, R_i, connected in parallel with a series combination of capacitances due to: the barrier (C_b), and the interface-2DEG distance and the density of states (C_x). Annulus area was 2.2x larger than disc area.

II. Experimental details

The device structure studied consisted of a barrier layer of 40 nm $Al_{0.85}Ga_{0.15}N$:Si≈10^{18} cm^{-3}, grown on a 550 nm thick UID $Al_{0.7}Ga_{0.3}N$ buffer that was regrown on an AlN/sapphire template. Schottky barrier electrical contacts of 10 nm Pt covered by 100 nm Au were deposited by e-beam evaporation on top of the barrier in the form of a disc (radius 840 μm), and surrounding annulus (inner radius 1240 μm, outer radius 1760 μm) , as shown in Figure 1. The structure forms back-to-back Schottky diodes where the annulus is operating in forward bias and the centre disc in reverse bias.

An Agilent E4980A Precision LCR Meter was used to measure the parallel capacitance and conductance of the disc-annulus test structure, with the annulus as the ground reference side and the oscillating bias applied to the disc contact. To mitigate against the effects of electrical parasitic elements, including stray capacitances, a four point Kelvin measurement was used whereby the disc and annulus Schottky contacts were simultaneously contacted with two probes each. Open and short calibrations of the measurement system were performed including the four point probes in place. This approach removed the effect of cabling and probes from our data, enabling

accurate C_P-G measurement over the wide frequency range used. Admittance-frequency curves were measured from 20 Hz up to 2 MHz at each disc voltage (V_{disc}), with an oscillation magnitude of 20 mV. V_{disc} was varied from 0 V to -8 V. The measured threshold voltage for the disc-annulus structure was approximately -7 V. We assume that the true threshold voltage for the heterostructure is within a few hundred mV of that value, once the small voltage drop across the forward biased annulus Schottky diode is subtracted. The full admittance-frequency-voltage (Y-f-V) measurement was repeated at wafer chuck temperatures from 25 °C to 75 °C.

Mobility was extracted from the Y-f-V measurements using an equivalent circuit model, as shown in Figure 1. This method uses the lateral resistance and charge density of the 2DEG to extract mobility and is especially sensitive to the device threshold and sub-threshold regions. The method used here differs from that reported in [5] by the addition of a series capacitance term to represent the annulus Schottky contact ($C_{annulus}$), a resistance to represent the ungated channel (R_{access}), and modification to the admittance of each element to account for the circular geometry of the test structure. Based on the demonstration in that paper and in [6] that there was an insignificant GaN/AlGaN heterojunction interface state density, it is assumed here that there are no interface states at the AlGaN/AlGaN heterojunction. There are likely to be bulk traps in the AlGaN barrier, which may add a background contribution to the admittance under reverse bias, however we expect their distorting effect on G/ω-f peak positions, discussed below, to be minimal.

$C_{annulus}$ was calculated from the unbiased 20 Hz disc-annulus capacitance measurement as a series combination using the areas of the two contacts: $C_{annulus} = C_{measured} \times A_{annulus} \times \left(\frac{1}{A_{disc}} + \frac{1}{A_{annulus}}\right)$. The total impedance was then $Z_{total} = Z_{annulus} + Z_{access} + Z_{disc}$. $Z_{annulus}$ is purely capacitive and assumed to be constant over the measurement voltage and frequency range (i.e. a high density 2DEG is always present under the annulus), and Z_{access} is purely resistive. Z_{disc} was constructed iteratively from parallel capacitance elements ($C_{b,i}$ and $C_{x,i}$ in series) and series resistances (R_i), as shown. The capacitance of each element of the Schottky disc region is comprised of three capacitances in series as outlined in [7]: (i) the barrier itself; (ii) an additional thickness (set at 1 nm) due to the separation of the 2DEG from the AlGaN/AlGaN interface; (iii) the capacitance from the 2DEG density which is limited by the finite electronic density of states, calculated using $A_i \times q \times n_{2DEG} / \frac{2kT}{q}$, where A_i is the area of the i^{th} element. This final term is due to the change in charge in the 2DEG as the applied voltage shifts the Fermi level [8]. The factor of 2 in (iii) was applied for the strong inversion region, changing to 1 in weak inversion where the 2DEG density is insufficient to screen the electric field [9]. The electrical permittivity of $Al_{0.85}Ga_{0.15}N$ was determined following [10]. The resistance of each element is given by $\frac{R_{sheet}}{2\pi} \ln\left(\frac{R_2}{R_1}\right)$, where R_2 and R_1 are the outer and inner radii of each element. R_{access} was found similarly. R_{sheet} was taken to be $\frac{1}{\mu Q}$, where Q is the areal carrier density (n_{2DEG}), and μ is the channel mobility. Q was determined by integrating the $C_{disc} - V$ curve formed from the 20 Hz capacitance measurement taken at each V_{disc} value, after subtracting the capacitance of the annulus. Therefore μ is the only free parameter in the fit.

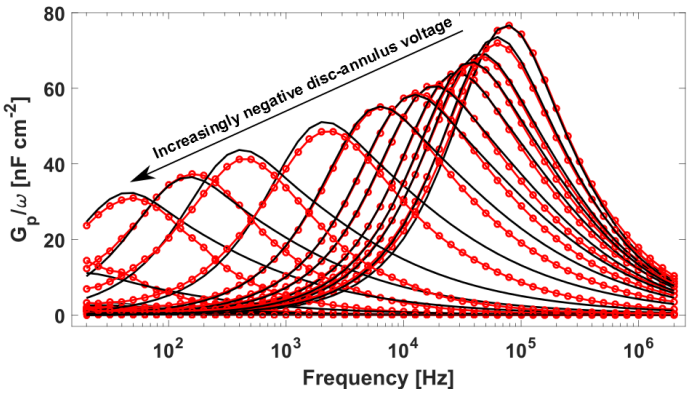

Fig. 2. G_p/ω vs. frequency for a subset of the disc voltages tested. The disc voltage was decreased from 0 V to -8 V in 50 mV steps. Model conductance curves (black lines) are constructed using the mobility found by fitting the experimental data (red circles).

The admittance of the model structure is given by $Y = \frac{1}{Z_{total}}$. The real component of the admittance is the conductance, which when plotted as $\frac{G}{\omega}$ against ω displays a characteristic peak for each V_{disc} tested [11], as shown in Figure 2. The fitting algorithm used the logarithm of the ratio of the peak positions for the measured and model curves as the optimisation target to be minimised. To determine the frequency of each peak an appropriately weighted Gaussian function was fitted to the curves and the position of its centre was taken as the peak in the $\frac{G}{\omega}$-frequency curve. A Gaussian function was chosen for computational efficiency in fitting the peak region of the model and data; it does not form part of our physical impedance model. μ was then adjusted to reduce the difference between the peak positions of the two curves, a new Z_{total} calculated, and the iteration repeated until the required tolerance was reached and μ had been found for the V_{disc} value. This procedure was repeated at each V_{disc} value, and at each temperature.

III. Results and Discussion

Taking the data in Figure 2 a peak mobility value of 155 cm^2/Vs at 25 °C, at n_{2DEG} = 5.1×10^{12} cm^{-2} corresponding to a voltage drop of -2.95 V across the barrier was determined for this structure. Hall mobility measurements using large area indium contacts corresponding to the unbiased case on the same wafer determined values of 135 cm^2/Vs at 9.9×10^{12} cm^{-2}; contactless sheet resistance using a Lehighton instrument and Hg-probe C-V measurements, again for the unbiased case, found 180 cm^2/Vs at 9.8×10^{12} cm^{-2}. For comparison our method measured a mobility of 122 cm^2/Vs at 9.51×10^{12} cm^{-2} for the unbiased case. The numbers are broadly in agreement; small differences may have arisen due to barrier thickness variations between the different wafer locations that each sample was taken from and the impact of any voltage drop across the annulus.

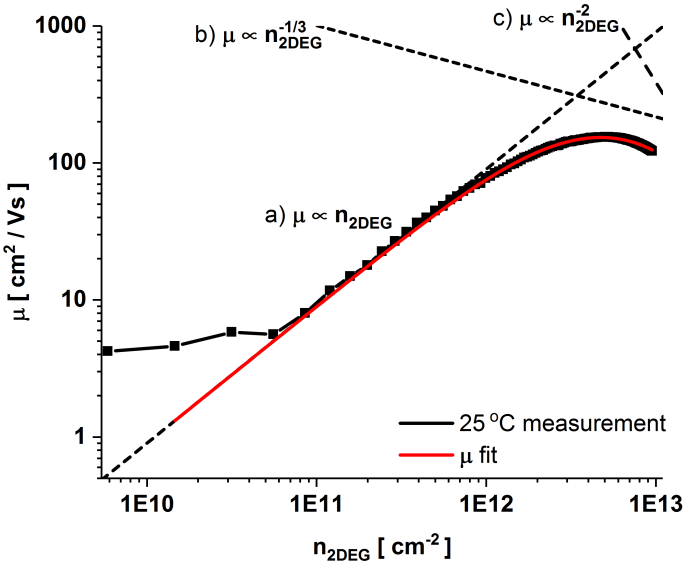

Fig. 3. Mobility as a function of n_{2DEG} at 25 °C. The kink at 4×10^{10} cm^{-2} is due to the change in expression for semiconductor capacitance used in weak and strong inversion regimes. Dashed lines represent mobility due to a) ionised defect scattering, b) alloy scattering, c) interface roughness scattering. The red line is a fit to the data of a function of a), b), and c) combined using Matthiessen's rule.

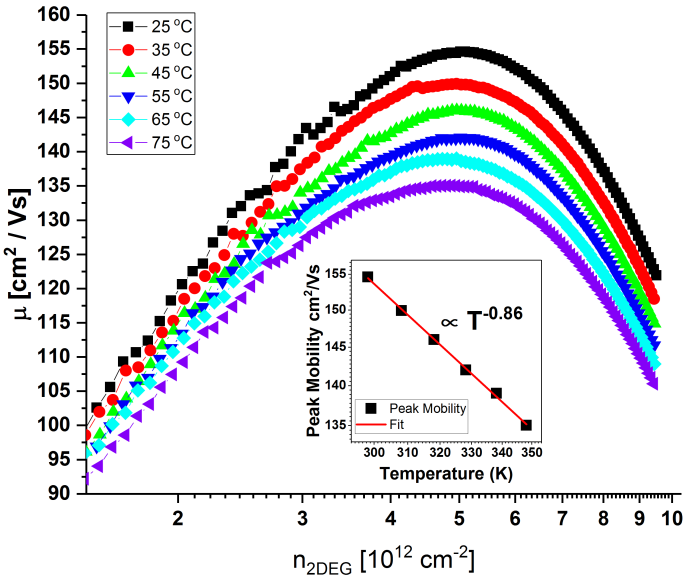

Fig. 4. Mobility plotted against n_{2DEG} centred around the maxima for each temperature value measured. Inset: Peak mobility plotted against temperature.

As shown in Figure 3, for densities below 10^{10} cm^{-2} the mobility becomes density independent at 4 cm^2/Vs due to the inability of the electrons in weak inversion to screen the scattering centres. The transition from weak to strong inversion occurred for carrier densities around 3×10^{10} cm^{-2}. The mobility then increases with increasing carrier density, following $\mu \propto n_{2DEG}^{0.88\pm0.02}$ from 10^{11} cm^{-2} up to around 10^{12} cm^{-2}. This is consistent with scattering by ionised defects being dominant, and increasingly screened by the carrier concentration in the channel [3], [4].

The mobility reaches a maximum at $\approx 5\times10^{12}$ cm^{-2} before falling. The mobility in this regime is expected to become limited by alloy scattering which varies as $n_{2DEG}^{-1/3}$ [12], since barrier and buffer materials are ternary alloys. Increasing n_{2DEG} also moves the charge distribution closer to the interface, increasing its limiting effect on mobility [13], suggesting an increasing importance of alloy scattering and interface roughness scattering with increasing 2DEG density, consistent with our data.

Summing ionised defect scattering, alloy scattering, and interface roughness via Matthiessen's rule produced an excellent phenomenological fit to the data, as shown in Figure 3. The fit suggests that between 1×10^{12} and 7×10^{12} cm^{-2} alloy scattering reduces the rate of increase of mobility with n_{2DEG}, but at higher concentrations interface roughness rapidly limits mobility. Removing the fitted interface roughness term suggests that a peak mobility of 177 cm^2/Vs at 7.8×10^{12} cm^{-2} could be obtained with increased interface smoothness.

The temperature dependence of the mobility is shown in Figure 4. The inset shows that peak mobility decreases as $T^{-0.86}$ over the temperature range tested. This temperature dependence is significantly reduced from what is expected for optical phonon scattering ($T^{-1.5}$) [14], and is closer to the $T^{-0.5}$ expected for alloy scattering [15]. A $T^{-0.7}$ to $T^{-0.85}$ dependence of alloy disorder scattering on temperature was found by Glicksman in Germanium-Silicon alloys [16] after removal of ionised defect and phonon mobility limits. The peak mobility temperature dependence is therefore further evidence in favour of alloy scattering being the mobility limiting factor in these $Al_{0.85}Ga_{0.15}N$ / $Al_{0.7}Ga_{0.3}N$ devices.

Over the 25 °C to 75 °C temperature range tested Schottky contact leakage did not adversely affect our measurements. Leakage current would increase as chuck temperature is increased, however as demonstrated in [11], its influence is easily distinguished as an increase in $\frac{G}{\omega}$ as measurement frequency is decreased. We expect that our technique should be suitable for use at higher operating temperatures, a regime where UWB heterojunction devices are of particular interest.

IV. Conclusions

It was shown that 2DEG mobility can be measured from weak inversion through to the unbiased case, in ultra-wide bandgap semiconductor AlGaN heterostructures, via a Y-f-V technique using only Schottky contacts. This technique may therefore be especially valuable for early feedback on new material developments. The maximum mobility values extracted using this technique are in good agreement with those measured by Hall measurement. Concentration-dependent mobility and temperature-dependent mobility at around 5×10^{12} cm^{-2} suggest that alloy scattering is presently limiting peak mobility in this material. Reducing interface roughness may however increase mobility to closer to 177 cm^2/Vs.

References

[1] J. Hudgins, "Wide and narrow bandgap semiconductors for power electronics: A new valuation," *Journal of Electronic Materials*, vol. 32, no. 6, pp. 471–477, June 2003, doi: https://doi.org/10.1007/s11664-003-0128-9.

[2] D. K. Schroder, *Semiconductor Material and Device Characterization*, 3rd ed. New Jersey, USA: Wiley, 2006.

[3] M. Manfra, S. H. Simon, K. W. Baldwin, A. M. Sergent, K. W. West, R. J. Molnar, and J. Caissie, "Quantum and transport lifetimes in a tunable low-density AlGaN/GaN two-dimensional electron gas," *Appl. Phys. Lett.*, vol. 85, no. 22, pp. 5278–5280, November 2004, doi: 10.1063/1.1827939.

[4] M. J. Manfra, K. W. Baldwin, A. M. Sergent, R. J. Molnar, and J. Caissie, "Electron mobility exceeding 160000 cm^2/V s in AlGaN/GaN heterostructures grown by molecular-beam epitaxy," *Appl. Phys. Lett.*, vol. 85, no. 22, pp. 5394–5396, November 2004, doi: 10.1063/1.1824176.

[5] W. M. Waller, M. J. Uren, K. B. Lee, P. A. Houston, D. J. Wallis, I. Guiney, C. J. Humphreys, S. Pandey, J. Sonsky, and M. Kuball, "Subthreshold Mobility in AlGaN/GaN HEMTs," *IEEE Transactions on Electron Devices*, vol. 63, no. 5, pp. 1861–1865, 2016, doi: 10.1109/TED.2016.2542588.

[6] M. Silvestri, M. Uren, and M. Kuball, "Dynamic transconductance dispersion characterization of channel hot carrier stressed 0.25μm AlGaN/GaN HEMTs," *IEEE Electron Device Letters*, vol. 33, no. 11, pp. 1550–1552, November 2012, doi: 10.1109/LED.2012.2214200.

[7] S. Takagi and A. Toriumi, "Quantitative understanding of inversion-layer capacitance in Si MOSFETs," *IEEE Transactions on Electron Devices*, vol. 42, no. 12, pp. 2125–2130, Dec 1995, doi: 10.1109/16.477770.

[8] A. Hartstein and N. F. Albert, "Determination of the inversion-layer thickness from capacitance measurements of metal-oxide-semiconductor field-effect transistors with ultrathin oxide layers," *Phys. Rev. B*, vol. 38, no. 2, pp. 1235–1240, July 1988, doi: 10.1103/PhysRevB.38.1235. [Online]. Available: https://link.aps.org/doi/10.1103/PhysRevB.38.1235

[9] J. Brews, "A charge sheet model of the MOSFET," *Solid-State Electronics*, vol. 21, no. 2, pp. 345–355, 1978, doi: https://doi.org/10.1016/0038-1101(78)90264-2.

[10] O. Ambacher, J. Majewski, C. Miskys, A. Link, M. Hermann, M. Eickhoff, M. Stutzmann, F. Bernardini, V. Fiorentini, V. Tilak, B. Schaff, and L. F. Eastman, "Pyroelectric properties of Al(In)GaN/GaN hetero- and quantum well structures," *Journal of Physics: Condensed Matter*, vol. 14, no. 13, p. 3399?3434, 2002, doi: https://doi.org/10.1088/0953-8984/14/13/302. [Online]. Available: stacks.iop.org/JPhysCM/14/3399

[11] W. M. Waller, S. Karboyan, M. J. Uren, K. B. Lee, P. A. Houston, D. J. Wallis, I. Guiney, C. J. Humphreys, and M. Kuball, "Interface state artefact in long gate-length AlGaN/GaN hemts," *IEEE Transactions on Electron Devices*, vol. 62, no. 8, pp. 2464–2469, August 2015, doi: 10.1109/TED.2015.2444911.

[12] G. Bastard, *Wave mechanics applied to semiconductor heterostructures*. Les Ulis Cedex, France: Jouve, 1988.

[13] J. Antoszewski, M. Gracey, J. Dell, L. Faraone, G. Parish, Y.-F. Wu, and U. Mishra, "Scattering mechanisms limiting two-dimensional electron gas mobility in $Al_{0.25}Ga_{0.75}N$/GaN modulation-doped field-effect transistors," *Journal of Applied Physics*, vol. 87, no. 8, pp. 3900–3904, April 2000, doi: https://doi.org/10.1063/1.372432.

[14] J. Blakemore, *Solid State Physics*, 2nd ed. Cambridge, UK: Cambridge University Press, 1985.

[15] J. W. Harrison and J. R. Hauser, "Alloy scattering in ternary III-V compounds," *Physical Review B: Condensed Matter and Materials Physics*, vol. 13, no. 12, pp. 5347–5350, June 1976, doi: 10.1103/PhysRevB.13.5347.

[16] M. Glicksman, "Mobility of Electrons in Germanium-Silicon Alloys," *Phys Rev*, vol. 111, no. 1, pp. 125–128, July 1958, doi: 10.1103/PhysRev.111.125.